Prabhakar R. Marur[1] *and Hareesh V. Tippur*[1]

Evaluation of Mechanical Properties of Functionally Graded Materials

Authorized Reprint from Journal of Testing and Evaluation, November 1998

REFERENCE: Marur, P. R. and Tippur, H. V., **"Evaluation of Mechanical Properties of Functionally Graded Materials,"** *Journal of Testing and Evaluation,* JTEVA, Vol. 26, No. 6, November 1998, pp. 539–545.

ABSTRACT: An experimental technique for evaluating the elastic properties of functionally graded materials (FGMs) is proposed. Ultrasonic pulse-echo measurements in conjunction with elastic impact testing permit determination of Young's modulus, Poisson's ratio, and the mass density of the material and its longitudinal variation. The details of the formulation of the technique and the implementation issues are discussed in this paper. These techniques have been applied successfully to evaluate the properties of a model functionally graded material.

KEYWORDS: ultrasonic pulse-echo measurement, elastic-impact technique (tap test), elastic constants evaluation, functionally graded materials

Nomenclature

g	Acceleration due to gravity
m	Mass of the specimen
m_1	Mass of the impactor
t	Time
t_d	Duration of impact
A	Acceleration
E	Young's modulus of the specimen
E_1	Young's modulus of the impactor
F	Contact force
R	Radius of spherical impactor
T_n	Natural period of the accelerometer
V_0	Initial impact velocity of the falling mass
V_l	Longitudinal wave velocity
V_s	Shear wave velocity
α	Approach
ν	Poisson's ratio of the specimen
ν_1	Poisson's ratio of the impactor
ρ	Mass-density of the specimen
ζ	Damping ratio of the accelerometer
ω_n	Natural frequency of the accelerometer

Introduction

In recent years, special composite materials collectively known as functionally graded materials (FGMs) have been introduced and extensively used in high-temperature applications [*1*]. In a typical FGM, the volume fractions of the constituents (usually two materials) are varied gradually, resulting in a medium with continuously graded physical properties at the macro level. This distinctive feature of the material can be exploited to obtain properties that are not offered by conventional materials. At present, FGMs are used mostly in high-temperature applications as mixtures of ceramic and metallic inclusions, where the graded layers considerably relieve the thermal stresses.

The spatial variation of elastic and physical properties necessitates application of elasticity of nonhomogeneous materials and poses a challenge in their material property evaluation, which forms the primary step in the experimental characterization of the FGM. Although the FGM is a mixture of two constituents, it is not analyzed in the sense of composites. A composite material is assumed to have a matrix in which inclusions of different elastic properties are embedded; although there is no restriction on the constituents to be isotropic, the mixture is assumed to be homogeneous and well dispersed throughout the material. In an FGM, the distinctive feature is the directional variation of the material properties along the length of the specimen. In essence, one could visualize an FGM as a sandwich of thin isotropic layers of varying material properties. This statement is made from the standpoint that in the absence of any preferred microstructural orientation, each wafer could be expected to behave isotropically. Although this presumption is open to question from a rigorous mathematical point of view, it seems reasonable physically and is supported by a similar observation made by Kinra and Ker [*2*], who have studied a composite of thin-walled glass spheres in a PMMA matrix.

The variation of the mechanical properties precludes the use of established evaluation techniques such as the rod-resonance approach [*3*], the acoustic-resonance method [*4*], etc. These techniques call for samples taken out from the specimen for material property evaluation, and the properties evaluated on the sample are assumed to represent the parent material. To apply these techniques for evaluation of an FGM, a large number of samples along the length of the specimen would need to be prepared and such a procedure would be cumbersome. Nondestructive methods such as impulse excitation techniques (IET) or free vibration tests [*5*] are also not suitable as the results pertain to the average value of the material properties. Hence, alternate approaches suitable to the problem in hand have to be looked into.

In this paper, a combination of pulse-echo measurements and tap tests is proposed to evaluate the mechanical properties of FGM. The ultrasonic wave velocity measurements are utilized for evaluation of the E/ρ ratio and Poisson's ratio and a novel application

Manuscript received 02/18/97; accepted for publication 04/07/98.
[1] Graduate student and associate professor, respectively, Department of Mechanical Engineering, Auburn University, Auburn, AL 36849.

of elastic impact theory to separate the variables in the E/ρ ratio. The formulation of elastic impact theory and application of the techniques in the evaluation of an epoxy-based FGM are discussed.

Ultrasonic Wave Velocity Measurements

The ultrasonic pulse-echo method is a well-established technique in which a piezoelectric transducer is coupled to the specimen to launch either a longitudinal or a shear wave and to measure the time required for the wave to travel through the thickness and return to the transducer. From the time-of-flight measurement and the knowledge of the thickness of the specimen, the wave velocities can be ascertained. By measuring the velocity of both the longitudinal and the shear wave propagation at the same location, the specific stiffness and the Poisson's ratio at that location can be evaluated as described below. The velocity of the longitudinal wave is given by

$$V_l^2 = \frac{E}{\rho} \frac{(1 - \nu)}{(1 + \nu)(1 - 2\nu)} \tag{1}$$

and the shear wave velocity is given by

$$V_s^2 = \frac{E}{\rho} \frac{1}{2(1 + \nu)} \tag{2}$$

After some algebra, it can be shown that

$$\nu = \frac{V_l^2 - 2V_s^2}{2(V_l^2 - V_s^2)} \tag{3}$$

$$\frac{E}{\rho} = V_l^2 \frac{(1 + \nu)(1 - 2\nu)}{(1 - \nu)} \tag{4}$$

If the Young's modulus or mass density could be ascertained by an independent measurement, the other property could be obtained from Eq 4. Measurement of density requires taking material from the specimen that renders it unsuitable for further mechanical tests. The other option of using microstructure analysis requires elaborate sample preparation. Hence, the possibility of nondestructive evaluation of the Young's modulus is explored using elastic-impact testing.

Elastic-Impact Test

Theoretical Formulation

Consider a large planar surface impacted by a small body, small enough to neglect its mass in comparison to the massive body as shown in Fig. 1. The conservation of linear momentum leads to the differential equation of motion

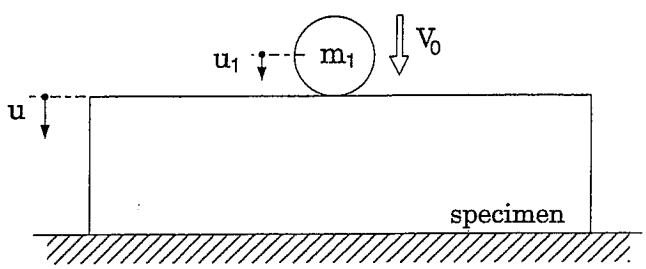

FIG. 1—*Impact of a falling mass on a massive body.*

$$-m\ddot{u} = -m_1\ddot{u}_1 = -\frac{mm_1}{m + m_1}(\ddot{u} - \ddot{u}_1) \tag{5}$$

where $(\cdot)$ implies differentiation with respect to time. Denoting the distance of approach of the bodies $(u - u_1)$ by α, and the ratio of masses by $k_1(= m + m_1/mm_1)$, conforming to the notation followed by Love [*6*], Eq 5 can be simplified as

$$-m\ddot{u} = -m_1\ddot{u}_1 = -\frac{1}{k_1}\ddot{\alpha} \tag{6}$$

The instantaneous contact force can be obtained from the elastic contact law as

$$F = k_2\alpha^q \tag{7}$$

where k_2 is a constant that depends on geometric and material properties of the bodies in collision, and q is the exponent. The exponent takes the value of 1.5 if Hertzian contact is assumed. The formulation is derived with q as a variable to make the results more general in view of the published results wherein exponents closer to unity [*7,8*] and greater than 1.5 are reported [*9*].

Equating Eqs 6 and 7 lead to the differential equation of motion

$$\ddot{\alpha} + k_1k_2\alpha^q = 0 \tag{8}$$

with the initial conditions $\alpha(0) = 0$ and $\dot{\alpha}(0) = V_0$. In deriving this equation, it is assumed that the coefficient of restitution is unity. This assumption is valid under certain restrictions on the choice of initial impact velocity V_0. In Ref *10,* it has been shown analytically that for V_0/V_1 less than 0.02%, the coefficient of restitution would be better than 0.996.

The above expression represents a solvable Emden-Fowler equation that has the implicit solution [*11*]

$$t = \int_0^{\alpha} \left[\frac{-2k_1k_2}{q + 1}\alpha^{q+1} + C_1\right]^{-1/2} d\alpha + C_2 \tag{9}$$

The constants C_1 and C_2 can be evaluated from the initial conditions as

$$C_1 = V_0^2,\ C_2 = 0 \tag{10}$$

and the velocity at any instant t can be obtained as

$$\dot{\alpha}^2 - V_0^2 = \frac{-2k_1k_2}{q + 1}\alpha^{q+1} \tag{11}$$

by differentiating Eq 9. The maximum approach α_m can be obtained as the approach at which the velocity becomes zero by assuming a reversible process, and it is given by

$$\alpha_m = \left[\frac{V_0^2(q + 1)}{2k_1k_2}\right]^{1/q+1} \tag{12}$$

The implicit solution for α can be rewritten in a simpler form using the expression for maximum approach as

$$t = \frac{\alpha_m}{V_0}\int_0^{\xi} \frac{d\xi}{\sqrt{1 - \xi^{q+1}}} \tag{13}$$

with

$$\xi = \frac{\alpha}{\alpha_m} \tag{14}$$

For $q = 1.5$, it has been noted in Ref *10* that a simple sine function well approximates the implicit solution given in Eq 13.

TABLE 1—*Values of η for different exponents, q.*

q	η
1	π
1.1	3.0954
1.2	3.0528
1.3	3.0135
1.4	2.9771
1.5	2.9423

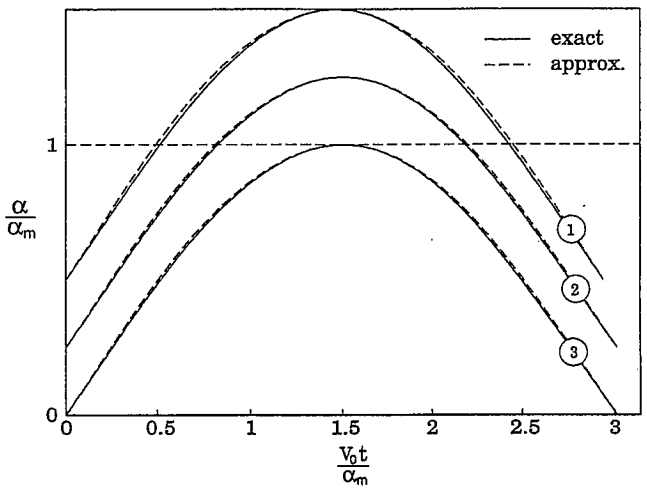

FIG. 2—*Comparison of the exact equation with half-sine approximation: (1)* q = *1.5; (2)* q = *1.3; (3)* q = *1.1. The curves are shifted in the ordinate for clarity.*

The equivalent sine function can be obtained by matching the time period of impact predicted by Eq 13 as

$$t_d = \frac{\alpha_m}{V_0}\eta \tag{15}$$

with

$$\eta = 2\int_0^1 \frac{d\xi}{\sqrt{1-\xi^{q+1}}} \tag{16}$$

The values of η for different values of q are given in Table 1. The expression for the equivalent sine function can then be given as

$$\alpha = \alpha_m \sin\left(\frac{\pi t}{t_d}\right) = \alpha_m \sin\left(\frac{\pi}{\eta}\frac{V_0}{\alpha_m}t\right) \tag{17}$$

For different values of q, the exact and approximate variations of α with time are shown in Fig. 2. From the figure it can be observed that the sine function well approximates the exact equation in each case, and the match is closer if the exponent approaches unity. For the linear case with the exponent at unity, the sine function is the exact solution.

From Eq 17, the expression for the contact force can be given as

$$F(t) = \frac{\pi^2 V_0^2}{\eta^2 k_1 \alpha_m}\sin\left(\frac{\pi}{\eta}\frac{V_0}{\alpha_m}t\right) \tag{18}$$

If the colliding body is spherical, and Hertzian collision is assumed to prevail, then k_2 is given by [6]

$$k_2 = \frac{4}{3}\sqrt{R}\left[\frac{1}{\frac{1-\nu_1^2}{E_1}+\frac{1-\nu^2}{E}}\right] \tag{19}$$

where R is the radius of the spherical impactor. In addition, if the mass of the impactor is small enough in comparison to the mass of the planar body, the parameter k_1 can be approximated as

$$k_1 = \frac{1}{m_1} \tag{20}$$

and the contact force can be expressed as

$$F(t) = m_1 \frac{1.14V_0^2}{\alpha_m}\sin\left(\frac{1.068V_0 t}{\alpha_m}\right) \tag{21}$$

To illustrate the variation of the impact force histories along the length of the specimen, a sample computation is carried out. Consider an FGM with its Young's modulus varying as shown in Fig. 3. For simplicity, the Poisson's ratio is assumed to be constant at 0.35. The impactor is a spherical steel ball of 4.75-mm radius with Young's modulus 209 GPa and Poisson's ratio 0.28. The simulated results for a specific case of impact velocity of 0.14 m/s (corresponding to a drop height of 1 mm) are shown in Fig. 4. It can be observed in the figure that both duration of impact and amplitude of the impact force vary distinctly with the elastic properties of the massive body. Hence measurement of either the duration of impact or peak force could be utilized for evaluating the elastic properties of the specimen. From Eq 21, it can be seen that for a given impactor and impact velocity, the impact force depends only on α_m, which in turn depends on E and ν of the sample. With the knowledge of Poisson's ratio obtained from the ultrasonic measurement, the longitudinal variation of the Young's modulus in the specimen can be evaluated.

Measurement of Impact Force

The impact force can be measured either by load sensors or by accelerometers. The direct force measurement seems unsuitable as the forces generated due to impact are very small, typically in the range of few newtons (see Fig. 4). In addition, the insertion of piezoelectric sensors (load washers, as popularly known) between the impactor and the specimen would result in perturbance of the stiffness at the contact surface. On the other hand, an accelerometer can be conveniently mounted on the distal side of the impacting mass, and the acceleration can be measured directly. In this study, a high-frequency sub-miniature accelerometer is used for the impact force measurement.

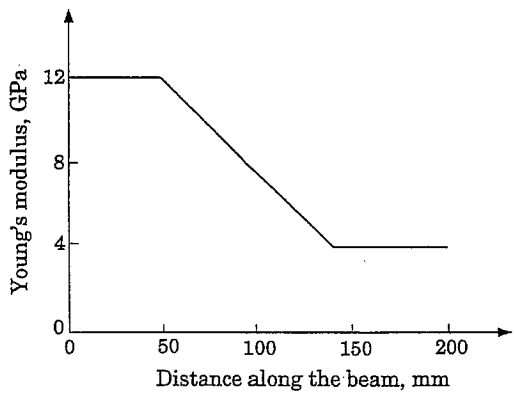

FIG. 3—*Longitudinal variation of Young's modulus.*

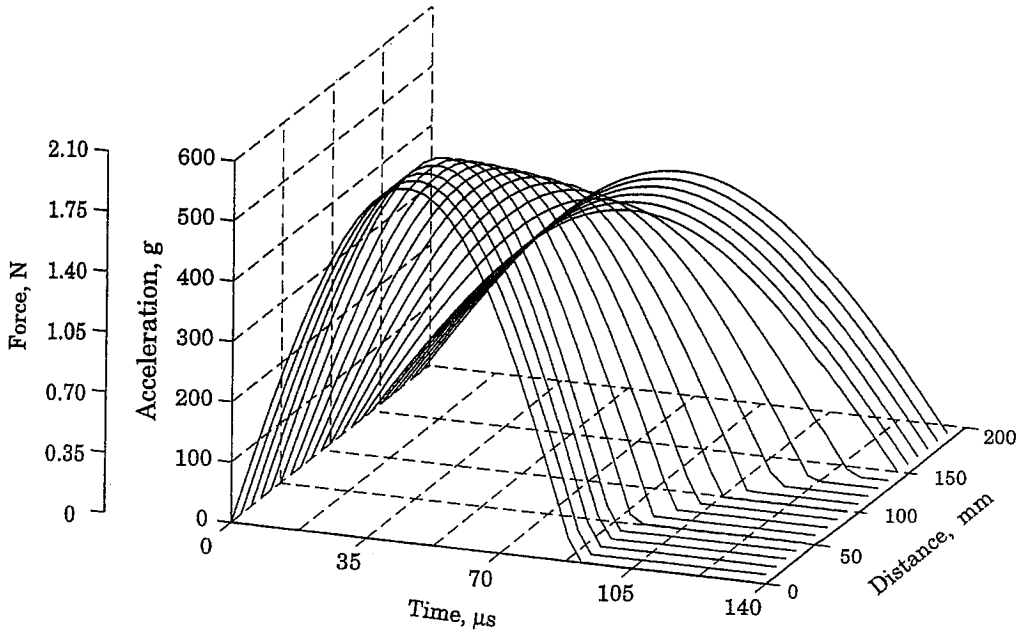

FIG. 4—*Computed impact force histories for the impact of 3.5-g mass on an FGM.*

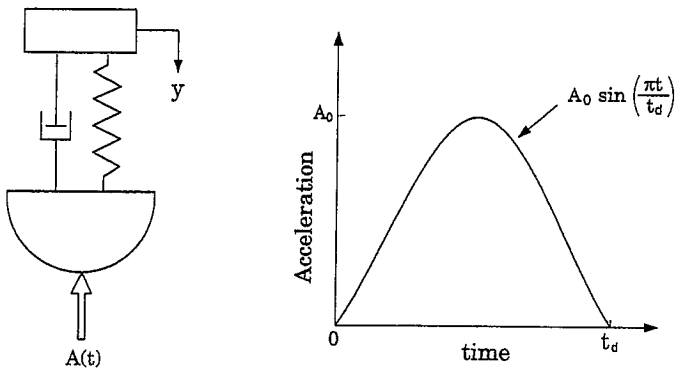

FIG. 5—*Idealized model of the accelerometer mounted on an impactor.*

The natural frequency of the accelerometer (or any dynamic force sensor, for that matter) needs to be carefully chosen with reference to the duration of impact to ensure proper results. Consider an idealized model of the accelerometer mounted on the impactor as shown in Fig. 5. Let the accelerometer be characterized by its natural frequency ω_n and damping ratio ζ, then the equation of motion for acceleration input corresponding to Eq 18 is given by

$$\ddot{y} + 2\zeta\omega_n\dot{y} + \omega_n^2 y = -A_0 \sin\left(\frac{\pi t}{t_d}\right)[H(t) - H(t - t_d)] \tag{22}$$

where $H(t)$ is the Heaviside step function, t_d is the duration of the half-sine input, and A_0 is the peak acceleration. Using the Laplace transform, the solution in terms of the dynamic magnification factor, DMF, can be given as

$$\frac{\omega_n^2 \ddot{y}}{A_0} = \frac{1}{\sqrt{(1 - r^2)^2 + (2\zeta r)^2}}\left[\sin\left(\frac{\pi t}{t_d} - \phi_1\right) - \frac{r}{\sqrt{1 - \zeta^2}} e^{-\zeta\pi t/rt_d} \sin\left(\sqrt{1 - \zeta^2}\,\frac{\pi t}{rt_d} - \phi_2\right)\right] \tag{23}$$

for $t < t_d$ and

$$\frac{\omega_n^2 \ddot{y}}{A_0} = \frac{-re^{-\zeta\omega_n t}/\sqrt{1 - \zeta^2}}{\sqrt{(1 - r^2)^2 + (2\zeta r)^2}}\left[\sin\left(\sqrt{1 - \zeta^2}\,\frac{\pi t}{rt_d} - \phi_1\right) + e^{\zeta\pi/r} \sin\left(\sqrt{1 - \zeta^2}\,\frac{\pi}{r}\left(\frac{t}{t_d} - 1\right) - \phi_2\right)\right] \tag{24}$$

for $t > t_d$,

where

$$r = \frac{T_n}{2t_d}$$

$$\phi_1 = \tan^{-1}\frac{2\zeta r}{1 - r^2}$$

$$\phi_2 = \tan^{-1}\frac{2\zeta\sqrt{1 - \zeta^2}}{1 - 2\zeta^2 - r^2}$$

To study the influence of the time duration of the half-sine pulse on the output from a given accelerometer, the response spectra for damped and undamped cases are derived. The response spectrum is obtained by differentiating the DMF equation with respect to t, setting it equal to zero, and substituting this time back in the DMF equation for every t_d/T_n ratio. The expressions are not given here for brevity, and details can be found in standard texts on vibration (for example, see Ref *12*.). The response spectra for undamped and damped cases are shown Fig. 6. It could be seen that in the undamped case, T_n must be at least an order less to reproduce the input acceleration to acceptable accuracy. However, with damping, the restriction on the natural frequency of the accelerometer is considerably relaxed. Since the response spectrum is obtained from a single point on the response curves, it does not convey full information about the sensor performance. A DMF time history for specific cases of t_d/T_n ratios must be plotted to study the effect of frequency ratios and damping on the sensor output. Sample plots for damped and undamped cases are shown in Fig. 7. The presence of damping results in exact reproduction of the input function, albeit the time delay that is inherent. Hence, it is suggested that the damped accelerometer with the period predicted by the response spectrum can be used effectively for the elastic impact force measurements.

The discussion is primarily centered around direct measurement of the impact parameters, which does not preclude using our accelerometer with an arbitrary characteristic to obtain the response and solving the inverse problem to reconstruct the input-forcing function. However, to retain simplicity and to avoid propagation of errors, it is desirable to use direct measurements.

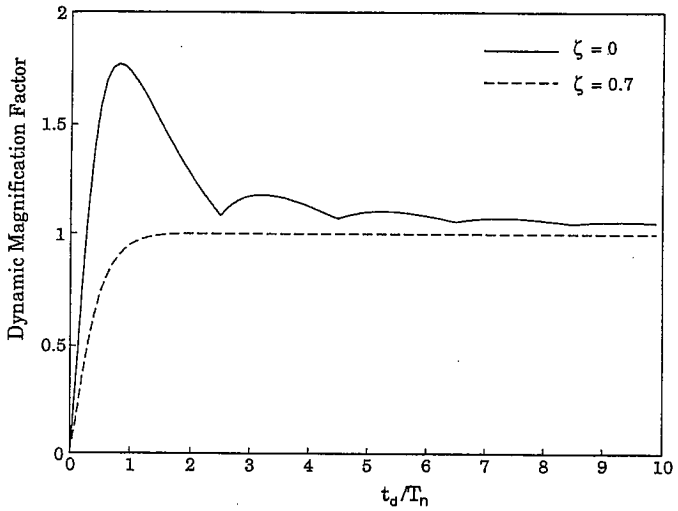

FIG. 6—*Damped and undamped response spectra for half-sine pulse input.*

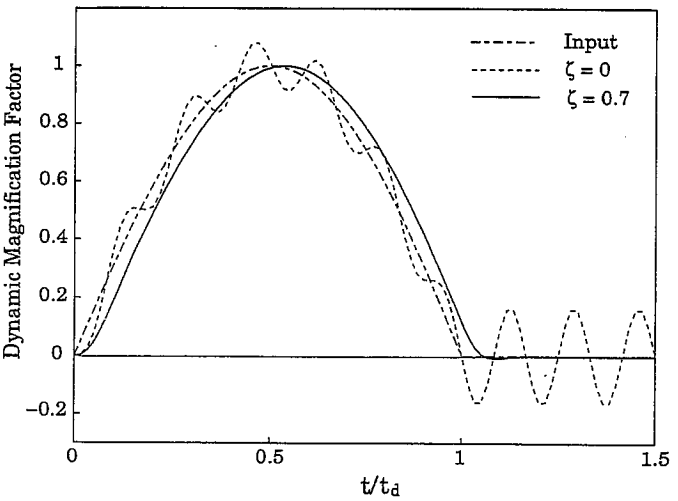

FIG. 7—*The damped and undamped DMF time histories for an accelerometer with a t_d/T_n of 6.*

Experimental Procedure

The techniques developed here were applied to evaluate the material properties of an epoxy-based functionally graded particulate composite at room temperature. An FGM specimen 160 by 25 by 6.3 mm was cast using uncoated solid glass spheres as inclusions in the epoxy matrix. The volume fraction of the glass beads was allowed to vary along the length of the specimen by using a gravity-assisted vertical casting process. The casting technique involves mixing glass beads (mean diameter of 50 μm) in a two-part slow-curing epoxy into a thick paste-like consistency (with epoxy to glass bead weight ratio of 1 : 2.35). The mixture is poured into an acrylic mold that is positioned vertically and allowed to cure for 24 h at ambient temperature and pressure. The slow curing rate of the epoxy offers enough time for the glass beads to move down through the curing matrix due to gravity. This results in an epoxy-rich top region and a bottom region with higher concentration of the glass spheres. In between these two regions, the volume fraction of the glass spheres varies almost linearly. This transition zone is usually on the order of 35 to 40 mm in length for the castings used in this study.

The gravity-assisted molding technique is quite successful in casting specimens of FGM with similar properties. Also, it must be noted that the properties are relatively constant in the thickness and width directions, resulting in a nonhomogeneous strip of material with unidirectional variation of the properties along the length.

The specimens were polished using fine emeries to make the surfaces parallel to each other and to remove asperities or air bubbles produced during the casting process. Then the ultrasonic wave speeds were measured at various locations along the length of the specimen. The longitudinal waves were launched using a transducer with a 3-mm diameter, and the shear waves were launched using a 6-mm-diameter transducer. In shear wave measurements, use of probes smaller than 6 mm resulted in large attenuation of the input waves, and the echoes were not distinct for accurate measurements. The pulse-echo data in terms of longitudinal and shear wave velocities are plotted in Fig. 8. From these wave velocities, the E/ρ ratio and Poisson's ratio were computed according to Eqs 3 and 4. The results are shown in Fig. 9. It can be observed that all the parameters have a linear spatial variation in the transition zone. The presence of the glass spheres results in stiffening of the matrix as expected and lowers the Poisson's ratio in the composite.

Subsequent to the pulse-echo measurements, elastic-impact tests were conducted at the same locations in the specimen. The impactor was made by grinding a 7.5-mm-diameter ball bearing to form a flat surface to facilitate accelerometer mounting. The total weight of the impactor, including the sensor, was 2.33 g, small compared

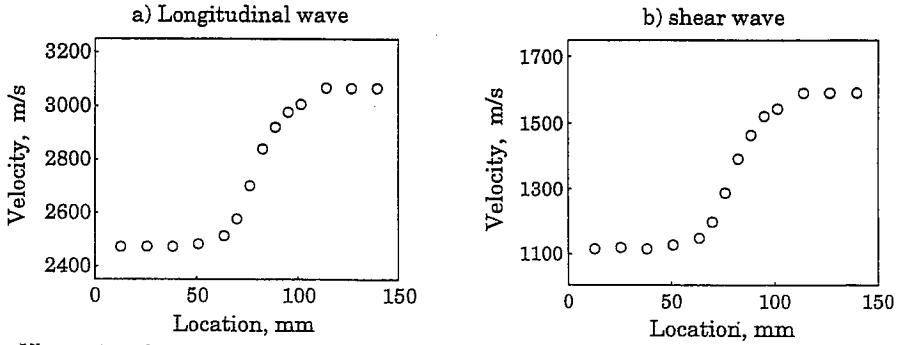

FIG. 8—*Ultrasonic pulse-echo data in terms of wave velocities:* (a) *longitudial wave speed;* (b) *shear wave speed.*

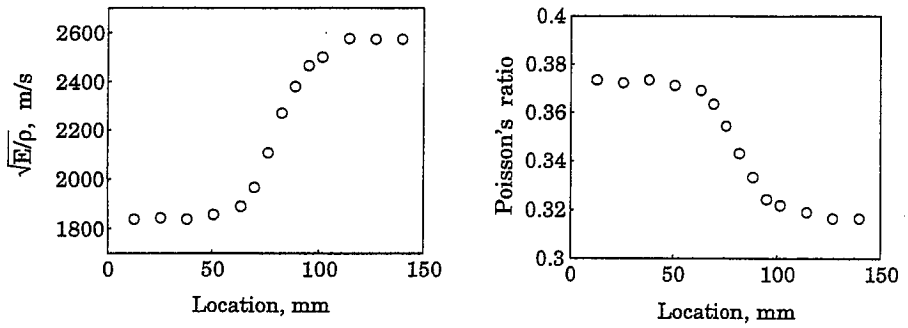

FIG. 9—*The longitudinal variation of specific stiffness and the Poisson's ratio derived from wave speed measurements.*

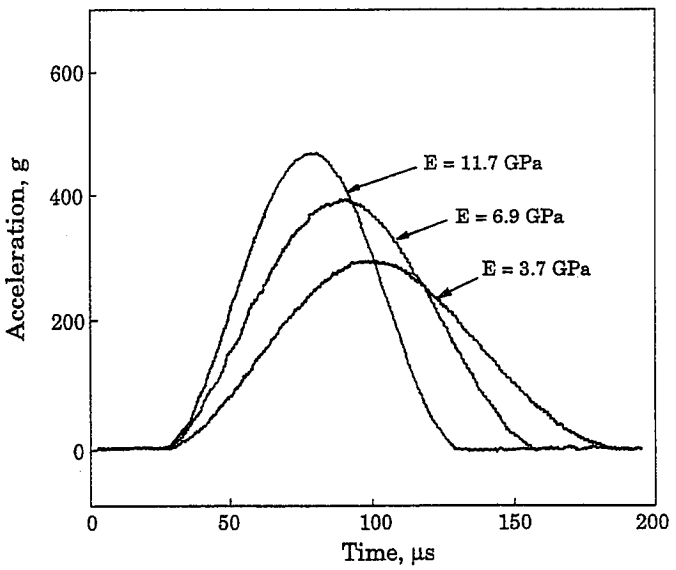

FIG. 10—*Typical measured acceleration-time histories.*

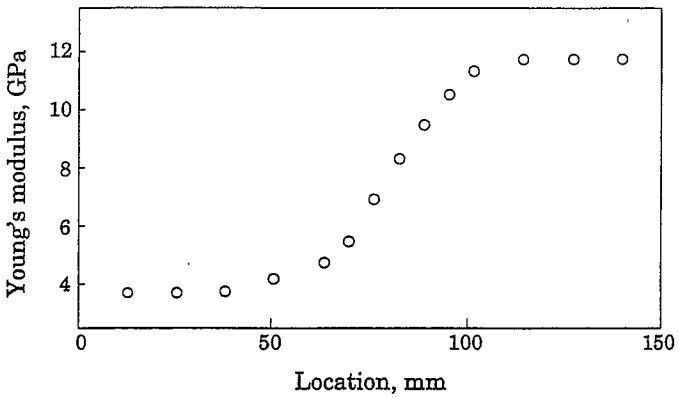

FIG. 11—*The Young's modulus measured by the elastic-impact test.*

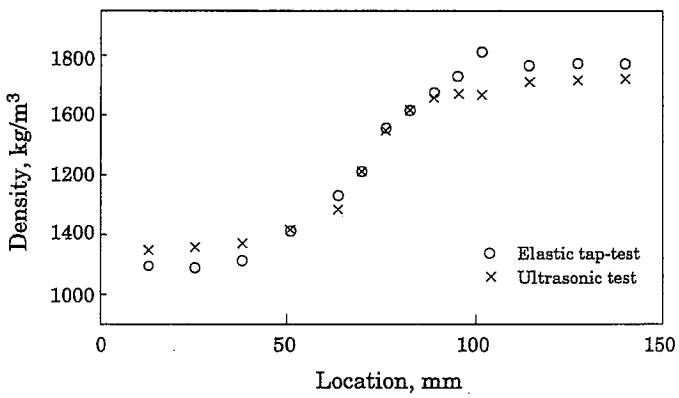

FIG. 12—*Comparison of measured mass-density with the estimated values.*

to the mass of the sample, which is 34.7 g. A sub-miniature, lightly damped accelerometer with a natural frequency of 120 kHz was used. The time period of the accelerometer was 1/6 the shortest duration of impact expected in the material. The output of the accelerometer was fed to a 100-MHz digitizing oscilloscope after charge-to-voltage conversion in the signal conditioner. The impactor was dropped with an initial impact velocity of 0.156 m/s (corresponding to a drop-height of 1.25 mm) using an electromagnet. The drop-height was set using a gage block of 1.25-mm thickness to ensure the accuracy of the setting and also the uniformity between the settings.

To ascertain the repeatability of the method, many trials were run on a PMMA specimen by tapping at different locations. The estimated Young's modulus was 3.5 GPa (with a standard deviation of 0.16 GPa), which compares well with the standard value for this material. The source of the spread in the measured values was the occasional aiding or restraining of the impactor motion by the accelerometer wiring, resulting in either high- or low-impact forces compared to the average values. Hence, in the testing of the FGM, a set of five measurements was taken at each location and the average was used in the estimation procedure. Some of the typical accelerometer outputs for the tests conducted on the FGM are shown in Fig. 10. The peak output was measured from the digital oscilloscope and used for computing the Young's modulus of the specimens as shown in Fig. 11. It must be remarked that time duration measurement is less preferable than the peak amplitude measurement as the edges of the sensor outputs were less distinctive to make accurate readings. The peak output was easy to measure and was repeatable. The peak output measurement offers an additional advantage in that a simple peak-hold amplifier could be used for the measurement instead of elaborate digitizing oscilloscopes or high-frequency data acquisition systems.

After completing the measurements, the specimen was cut into thin pieces and the density of each piece was measured. The measured data are compared with the estimated values in Fig. 12. It can be seen that in spite of the many simplifying assumptions made in the formulation of the tap test and about the behavior of the FGM, the match is reasonably good. The density is underestimated

in the epoxy-rich region by 5% and overestimated in the glass-reinforced side of the specimen by about 3%. Since the density is estimated by combining the experimental data from two distinctly different methods, especially operating at different excitation frequencies, the discrepancy could originate from many possibilities. For example, in the glass-bead–rich region of the specimen, the ultrasonic wave scattering is assumed to be negligible in the formulation. And in the epoxy-rich region, the Young's modulus is assumed to be invariant in both ultrasonic measurement and tap tests, although the operating frequencies are different. With refinement of the theory by accounting for the influence of the different factors mentioned, this technique can be evolved into an accurate material property evaluation method.

Conclusions

A combination of pulse-echo measurements and elastic-impact testing is proposed for the determination of mechanical properties of FGM. The technique is nondestructive and suitable for evaluating the material properties on a per-sample basis. The techniques developed here are applied to measure the properties of an epoxy-based, glass-sphere filled particulate composite with a linearly graded transition zone. The estimated material properties compare rather well with the measured data, validating the proposed method.

Acknowledgments

The authors would like to thank NSF (Grant No. CMS 9622055) and ARO Solid Mechanics Program (Grant No. DAAG55-97-1-0110) for supporting the research. The first author would like to thank the College of Engineering at Auburn University for providing support in his work through the 1996 Research Initiative Program.

References

[1] Holt, J. B., Koizumi, M., Hirai, T., and Munir, Z. A., Eds., "Functionally Graded Materials," *Ceramic Transactions,* Vol. 34, American Ceramic Society, Westerville, OH, 1993.

[2] Kinra, V. K. and Ker, E., "Effective Elastic Moduli of a Thin Walled Glass Microsphere/PMMA Composite," *Journal of Composite Materials,* Vol. 16, 1982, pp. 117–138.

[3] Read, R. D. and Ledbetter, H., "Elastic Properties of Boron-Aluminum Composite at Low Temperatures," *Journal of Applied Physics,* Vol. 48, 1977, pp. 2827–2831.

[4] Ledbetter, R. H., Fortunko, C., and Heyliger, P., "Orthotropic Constants of a Boron-Aluminum Fiber Reinforced Composite: An Acoustic-Resonance-Spectroscopy Study," *Journal of Applied Physics,* Vol. 78, 1995, pp. 1542–1546.

[5] Wolfenden, A., Harmouche, M. R., Blessing, G. V., Chen, Y. T., Terranove, P., Dayal, V., Kinra, V. K., Lemmens, J. W., Philips, R. R., Smith, J. S., Mahmoodi, P., and Wann, R. J., "Dynamic Young's Modulus Measurements in Metallic Materials; Results of an Interlaboratory Testing Program," *Journal of Testing and Evaluation,* Vol. 17, 1989, pp. 2–13.

[6] Love, A. E. H., *Theory of Elasticity,* Dover Publications, New York, 1944.

[7] Nash, G. E. and Lange, E. A., "Mechanical Aspects of the Dynamic Tear Test," *Journal of Basic Engineering,* Vol. 91, 1969, pp. 553–543.

[8] Marur, P. R., "An Engineering Approach to Dynamic Analysis of Notched Beams by Conventional Beam Elements," *Computers and Structures,* Vol. 59, 1996, pp. 1115–1120.

[9] Sun, C. T. and Yang, S. H., "Contact Law and Impact Responses of Laminated Composites," NASA-CR-159884, 1980.

[10] Hunter, S. C., "Energy Absorbed by Elastic Waves During Impact," *Journal of Mechanics and Physics of Solids,* Vol. 5, 1957, pp. 162–171.

[11] Polyanin, A. D. and Zaitsev, V. F., *Handbook of Exact Solutions for Ordinary Differential Equations,* CRC Press, NY, 1995, pp. 241–250.

[12] Jacobsen, L. S. and Ayre, R. S., *Engineering Vibrations,* McGraw-Hill Book Co., NY, 1958, pp. 160–187.